Analyst

Quantitative determination of protein molecular weight with an acoustic sensor; significance of specific versus non-specific binding

Journal:	*Analyst*
Manuscript ID:	AN-ART-04-2014-000616.R1
Article Type:	Paper
Date Submitted by the Author:	02-May-2014
Complete List of Authors:	Mitsakakis, Konstantinos; U. Freiburg, Microsystems Engineering Tsortos, Achilleas; FO.R.T.H, Institute of Molecular Biology & Biotechnology Gizeli, Electra; FO.R.T.H, Institute of Molecular Biology & Biotechnology

A multi-analyte acoustic biosensor determines the molecular weight of proteins via the phase change of the acoustic signal

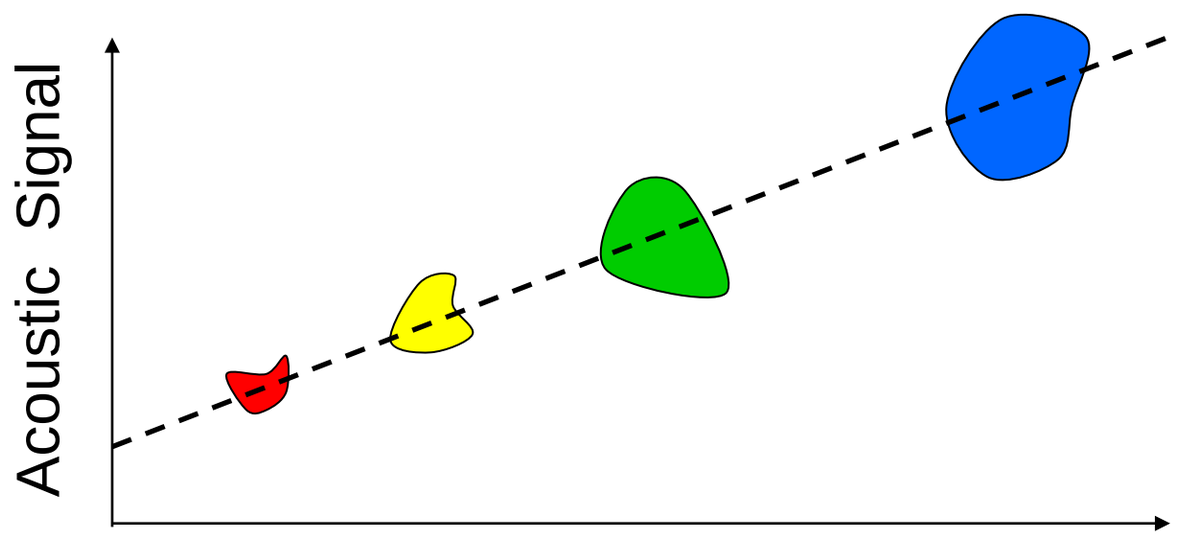

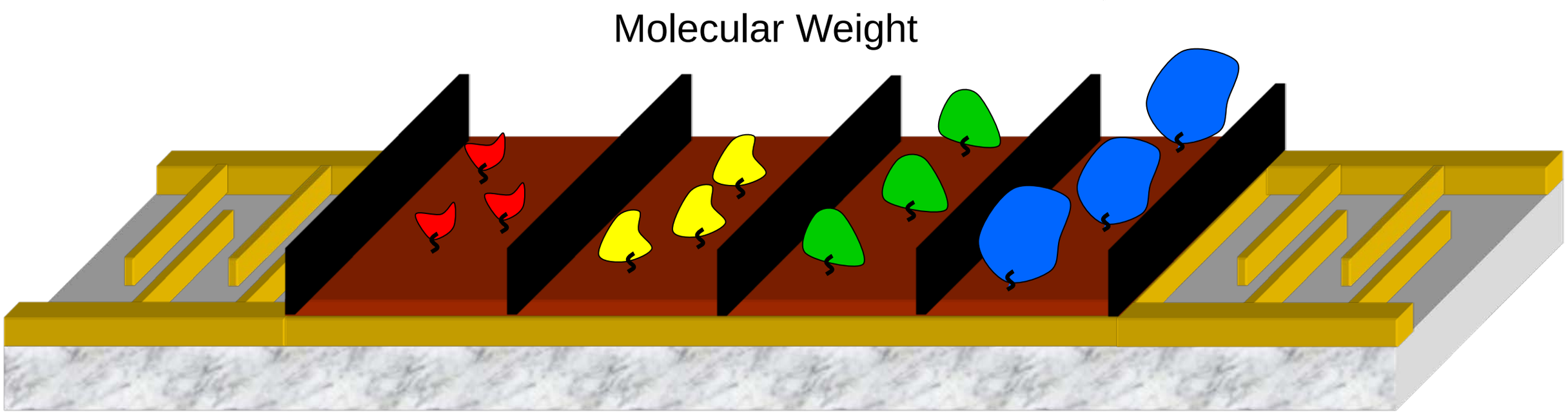

Cite this: DOI: 10.1039/c0xx00000x

www.rsc.org/xxxxxx

ARTICLE TYPE

Quantitative determination of protein molecular weight with an acoustic sensor; significance of specific versus non-specific binding

Konstantinos Mitsakakis,[a,b,§] Achilleas Tsortos*[a] and Electra Gizeli*[a,c]

Received (in XXX, XXX) Xth XXXXXXXXX 20XX, Accepted Xth XXXXXXXXX 20XX

DOI: 10.1039/b000000x

Surface acoustic wave sensors with integrated microfluidics for multi-sample sensing have been implemented in this work towards the quantitative correlation of acoustic signal to the molecular weight of surface bound proteins investigating different interaction/binding conditions. Results are presented for: (i) four different biotinylated molecules (30≤Mw≤150 kDa) specifically binding to neutravidin; (ii) the same four non-biotinylated molecules, as well as neutravidin, adsorbing on gold; and (iii) four cardiac marker proteins (86≤Mw≤540 kDa) specifically binding to their homologous antibodies. Surface plasmon resonance was employed as an independent optical mass sensor. A linear relation was found to exist between the phase change of the acoustic signal and the molecular weight of the proteins in both cases of specific binding. In contrast, non-specific binding of proteins directly on gold exhibited no such linear relation. In all three cases ΔPh was correlated to the bound mass per area. The underlying mechanism behind the different behavior between specific and non-specific binding is discussed by taking into account the geometrical restrictions imposed by the size of the specific biorecognition molecule and corresponding bound protein. Our results emphasize the quantitative nature of the phase of the acoustic signal in determining the Mw (in case of specific binding) with an accuracy of 15% and mass of the bound proteins (in all cases), as well as the significance of the biorecognition molecules in deriving molecular weight acoustic or optical detectors.

Introduction

The majority of transducer-based biosensors examine biomolecular processes from the viewpoint of detecting whether an interaction takes place, evaluating the bound mass and/or analyzing the affinity and kinetics of an interaction pair.[1-3] Acoustic sensors exceed the limits of mere analytical detection due to the nature of the sensing principle. Apart from their implementation in material characterization,[4,5] rheology,[6-8] and bio-analytical chemistry,[9-14] acoustic sensors have been used in biophysical studies[15-17] to translate the acoustic signal into a wide range of information, varying from the viscoelastic characteristics of bio-films to the molecular properties of discretely bound biomolecules. The former would normally refer to the complex shear modulus of a biological layer, which, when combined with mass-sensitive optical techniques, is used to derive the layer's thickness. [18,19] In addition, the film approach has been applied for monitoring changes in the structure of the surface-attached layer and qualitatively relate them to the conformation or organization of the molecules comprising the film.[20-24] A recently developed molecular approach has advanced the biophysical characterization of biomolecules with acoustic wave sensors by correlating the acoustic signal to the intrinsic viscosity of biomolecules, and, furthermore, to their shape and size.[25-29] Using a different approach but again towards molecular sensing, information related to the hydrodynamic water bound per DNA molecule was obtained.[30] In all the above cases, surface acoustic wave (SAW) devices as well as their counterpart, quartz crystal microbalance (QCM) have been used in experimental setups that acquire two measurements, namely the phase (*Ph*) or frequency (*F*) and the amplitude (*A*) or energy dissipation (*D*) of the wave. The dependency of the above two measurements on the mass and mechanical-viscoelastic properties of the bound matter is the reason behind the plethora of information derived with these systems, making acoustic wave sensors a powerful tool in biophysical studies.

In the current work we concentrate mainly on the mass-sensitive phase signal of a Love mode SAW-type device. First we address experimentally the on-going question of what do acoustic waves sense when proteins are attached to the surface; moreover, we explore for the first time acoustic response dependency on the molecular weight of bound proteins. While protein films at high surface coverage/saturation are normally treated as viscoelastic films,[31-33] we establish experimental protocols that allow the direct correlation of the acoustic signal to the molecules' intrinsic property of *Mw*. In fact, as the *Mw* determination often requires tedious and time and sample consuming chromatography-based procedures, a quick and accurate analysis is indeed significant for industry. In parallel to the Love mode SAW sensor, surface plasmon resonance (SPR) measurements were used as a complement[34,35] and strongly supported the drawn conclusions.

This study reveals the significance of surface architecture in controlling the number of bound molecules and highlights differences in signal response due to specific versus non-specific binding.

Experimental

Materials

Three sets of biomolecules were employed in this work: (i) set #1: biotinylated molecules (from Sigma), namely: protein G (b-PrG, 30 kDa), protein A (b-PrA, 42 kDa), bovine serum albumin (b-BSA, 66 kDa), and immunoglobulin G (b-IgG, 150 kDa); (ii) set #2: non-biotinylated molecules: neutravidin (Neu, 60 kDa) from Pierce, protein G (PrG, 30 kDa) from Calbiochem, protein A (PrA, 42 kDa) and bovine serum albumin (BSA, 66 kDa) from Sigma, and immunoglobulin G (IgG, 150 kDa) from Unilever Research, UK; (iii) set #3: cardiac markers from HyTest Ltd: recombinant creatine kinase MB (CK-MB, 86 kDa), human C-reactive protein (CRP, 125 kDa), human plasma D-Dimer (D-Dimer, 195 kDa), and pregnancy-associated plasma protein A (PAPP-A, heterotetrameric complex, 540 kDa), and their homologous monoclonal antibodies (Ab): anti-CK-MB (Santa Cruz Biotechnology, Inc.); mouse anti-human CRP, mouse anti-D-dimer, and mouse anti-human PAPP-A from HyTest Ltd. The solutions of all experimental sets were prepared in phosphate buffered saline (PBS), at pH 7.4 and experiments were carried out at 25 ºC.

Love wave acoustic device

The biosensing component is a dual-device SAW biochip (Fig. 1(a)), based on a quartz piezoelectric substrate. Two sets of gold interdigital transducer electrodes (IDTs) are photolithographically patterned on quartz (gold thickness 100 nm, with an intermediate 20 nm thick Cr layer for adhesion purposes). The IDT periodicity (32 μm) defines the operating frequency f = 155 MHz and the penetration depth $\delta \approx 50$ nm, within the liquid medium. The sensing area confined between the two IDT sets was also coated with a gold layer in order to prevent acoustoelectric interactions. The sensor operated in a Love wave mode[36] with a 0.70 μm thick polymethylmethacrylate (PMMA) film on the device (covering the IDTs and sensing area). The PMMA solution (14% w/w) was prepared in 2-ethoxyethyl acetate (>99%, Aldrich) and spin-coated on the device chip at 4,000 rpm for 60 s (P6700, Specialty Coating Systems Inc.) followed by thermal solidification at 195 ^{o}C for 2 h. A gold film (20 nm) was sputter coated (Bal-Tec SCD 050) on top of the PMMA (only over the sensing area) to investigate biomolecular adsorption. This device configuration was the optimum in terms of sensitivity and reproducibility, as decided upon a thorough parametric study of twelve different configurations.[37] The regeneration of the sensor surface between experiments was achieved by means of mild air plasma treatment (Harrick Scientific Corp.) for 5 min at 600 mTorr chamber pressure.

Acoustic measurements and experimental setup

The detection principle of acoustic sensors is based on the interaction of acoustic waves with the probed material and allows the label-free detection of biological species. Detection occurs when a loaded material and/or a particular process taking place on the device surface result in altering the wave characteristics, namely its phase and amplitude. The former is mainly related to adsorbed/deposited mass whereas the latter is related to energy loss via dissipation mechanisms.[4] Due to the piezoelectric nature of the sensors and the transformation of the acoustic wave into electric signal, the changes in wave quantities are measured in terms of phase (ΔPh) and amplitude (ΔA) changes of the electric signal. For the continuous monitoring of ΔPh the biochip was connected to an HP 8753ES Network Analyzer with a switch control unit (Agilent 3499A); data were collected every 30 s.

Microfluidics-on-SAW (μF-on-SAW)

A flow-through system was employed in all experiments taking advantage of microfluidics (Fig. 1(b)). The microfluidic module, facilitating multi sample probing, was made of polydimethylsiloxane (PDMS, Dow Corning Corp.) by means of rapid prototyping and replica molding (soft lithography).[38] The module, which was reversibly attached on the device to ensure reusability, divided the total device sensing area of ~7.44 mm^2 into four equal-area domains of ~1.76 mm^2 each. The module contact with the sensor did not cause significant damping (less than -30 dB in air after module attachment) due to the thin-walled microchannels. Due to the smaller area per domain the absolute signal was proportionally smaller than that acquired using the entire sensor surface; however, the sensitivity remained the same, as it depends on the sensor structural characteristics, and the reproducibility was near 90% (due to the microfluidic nature of the setup). More details on the design and fabrication procedure can be found in previous work.[39] For fluid handling, a syringe pump (HARVARD PHD2000) was used with the μF-on-SAW configuration at constant flow rate 5 μl/min. The multi-sample injection was sequential, not parallel, so as to avoid signal interference from simultaneous injection of different analytes in the microchannels.

SPR device and instrumentation

For the optical measurements a Reichert SR7000 SPR apparatus was used, operating at 780 nm. The sensor chip (XanTec) was a gold-coated (50 nm) glass slide. Surface regeneration was achieved with air plasma treatment. The optical signal (change of micro refractive index units, μRIU, upon adsorption and/or binding) is directly proportional to the surface mass density via the following relation provided by the manufacturer: 1 ng/mm^2 =1610 μRIU. Data were collected every 5s. The SPR apparatus was connected with a peristaltic pump for constant flow rate 5 μl/min.

Results

Specific binding of biotinylated proteins to neutravidin

In the first set of experiments we used neutravidin as the biorecognition molecule. It was first physisorbed (200 μg/ml) on the gold sensor surface and following rinsing, BSA (1 mg/ml) was used as blocking agent in order to prevent non-specific binding. Biotinylated molecules, namely, b-PrG, b-PrA, b-BSA and b-IgG (Mw 30 to 150 kDa) were applied on the neutravidin functionalized Love wave device surface at a concentration of 50 μg/ml which corresponds to the plateau region of their corresponding binding curves, thus, ensuring surface saturation.[40]

In Fig. 2(a) the real time phase change is shown during the binding (the neutravidin adsorption and BSA blocking steps that preceded the specific binding are not included in Fig. 2(a)). The specificity of the interaction was confirmed by observing no signal change upon application of all four non-biotinylated proteins to the neutravidin layer. To complement acoustic results, the same experiments were carried out under identical conditions (protein batch, buffer, protein concentration, etc.) using an SPR optical biosensor (data shown in Figure S-1).

Non-specific adsorption of proteins on Au

The same four proteins used in the neutravidin experiments were applied in their non-biotinylated form on gold and the phase was again recorded during their adsorption (Fig. 2(b)). These proteins were applied at a concentration of 100 μg/ml (in PBS at 25°C), a quantity sufficient to result in full coverage.[38] PBS rinsing followed each adsorption step. SPR was also used to follow the surface coverage in real time (Figure S-2(a)).

Specific binding of cardiac markers to immobilized antibodies

The specific binding of protein set #3 (four cardiac markers) with a *Mw* between 86 and 540 kDa was also followed in real time (Fig. 2(c)). First, antibody immobilization (20 μg/ml) was achieved on a PrG (500 μg/ml) covered gold surface. Then the cardiac markers were flowed over the μF-on-SAW device at saturation levels (20 μg/ml) and the real time binding was recorded; BSA (1 mg/ml) was again used as blocking agent prior to the injection of the cardiac markers. The real time curves in Fig. 2(c) indicate only the signal change due to the cardiac markers specific interaction; the preceding surface immobilization steps are shown in Figure S-2(b). Non-specific binding was not observed as reported before.[41]

Discussion

The rationale behind this work was to exploit the mass-sensitive signal ΔPh of an acoustic device towards the development of a sensor for probing the *Mw* of proteins. In order to do so, one has to assume that the acoustic mass sensed by ΔPh is the same for all proteins, regardless of their size and method of attachment. It is known that:

$$m = N \times Mw/N_A \quad (1)$$

where *m*, and *N* are the mass and number of molecules per unit area, respectively and N_A is the Avogadro number. If we assume that ΔPh is proportional to *m*, then based on eqn (1) one would expect to be able to compare directly ΔPh to *Mw* if the number of molecules *N* is constant and, thus, incorporated in the slope of the ΔPh vs. *m* plot (see below). Therefore, the relevant question was whether it is possible to develop a biorecognition surface that provides good control on the number of bound molecules.

Protein binding to neutravidin and gold

We used standard surface chemistry to bind specifically biotinylated molecules to a neutravidin modified surface. From Fig. 2(a) we measured the phase change at saturation (following buffer rinsing) for each protein. Examining the relation of ΔPh detected during the specific interaction as a function of the molecules' *Mw*, a linear correlation is observed (Fig. 3(a), circles). The linear trend was confirmed via experiments with SPR under the same conditions (Fig. 3(b)). To further investigate the importance of specific binding to the number of neutravidin-attached molecules, we calculated from Fig. 2(b) the phase change that corresponds to the adsorption of the same non-biotinylated proteins directly to the gold surface. Interestingly, Fig. 4 shows that in this case no trend exists between ΔPh and *Mw*; again, SPR data are in agreement with SAW. It is easy to notice some striking features: (a) while neutravidin and BSA have almost the same *Mw*, $\Delta Ph_{neu} \cong 1.5 \times \Delta Ph_{BSA}$; (b) PrA exhibits a very low signal, disproportional to its *Mw*; (c) even though there is significant difference in the *Mw* of IgG, Neu and PrG the signal change is not correspondingly different. Qualitatively, the SAW and SPR lines in Fig. 3(a,b) parallel each other; the relative magnitude (ratio) between the two signals (SPR/SAW signal) is of the order of 520±20 (deg/μRIU) for the biotinylated proteins on neutravidin. The same signal ratio for the adsorbed proteins on gold, derived from Fig. 4, is of the order of 620±20 (except for PrG which is slightly off).

In order to examine if this depicts some underlying differences between optically and acoustically sensed mass in the two experiments, we used SPR data from both experimental sets to calculate surface mass density (*m*) of bound proteins and correlate it to ΔPh. Fig. 5 indicates a linear correlation between ΔPh and the amount of bound mass per area; similar combined SAW/SPR experiments have been performed before but with a limited number of biomolecules.[35] The linear fit gives:

$$\Delta Ph = 2.2\, m + 0.44 \ (R^2 = 0.92) \quad (2)$$

The linear correlation observed in Fig. 5 for all 5 proteins provides new insight in the nature of acoustic sensing and merits some further analysis. While the Sauerbrey equation[42] is used to quantify the amount of deposited mass and speaks about a linear correlation between ΔF (or ΔPh) and Δm, this applies strictly to the deposition of a homogeneous rigid film. Protein biophysicists are dealing with the deposition of individual molecules or aggregates (but not films) which are acoustically "soft" and exhibit energy dissipation. Moreover, several works support the theory that protein mass sensed with acoustic sensors in the presence of liquid does not reflect only on the dry mass of the bound protein (sensed with optical techniques such as SPR) but also includes amounts of trapped water.[31,43,44] These works have shown that for individual protein adsorption a correlation exists between acoustic and optical mass; however, to our knowledge, no data exist correlating ΔPh to *m* of a group of proteins adsorbed to the sensor surface which are also attached using two different methods. Such an approach is similar to the one followed by researchers in the early stage of SPR development where the linear correlation between SPR signal and surface concentration of three model proteins was established.[45] The linear relationship observed here, is not self-evident when one examines different proteins. Within the frame of "trapped water" theory,[31] one could expect that different proteins may exhibit different acoustic mass while having the same optical mass density. However, Fig. 3 clearly indicates that the acoustic and optical mass of the 5

proteins adsorbed in this case is directly analogous, despite of the protein size, shape, viscoelasticity [a] and surface density or even attachment mode. This conclusion is important in order to, subsequently, attempt to correlate *ΔPh* to the molecular mass of each protein.

A point of interest here is that the line described by eqn (2) does not go through zero, as one would expect. This observation is consistent with other data in our lab, which might suggest another underlying coupling mechanism between a liquid sample and the acoustic wave (both in the case of SAW and QCM), even in those cases where no obvious mass deposition or viscosity/density changes take place. Although the effect of the electrical properties and number of attachment points of the bound mass play a role, it is not clear to us and the community as to why it occurs. For this reason, we decided to use eqn (2) in its current form, i.e., without forcing it to pass through zero.

As seen in Fig. 3(a,b) for the case of specific binding of biotinylated molecules and at saturation, apparently, *N* can be incorporated in the slope thus the number of molecules bound to the neutravidin-modified surface is a constant; this is not the case for non-specific adsorption. Based on eqn (1) though one would expect that the linearity not observed between *ΔPh* and *Mw* in the case of physisorption on gold, could be recovered if *ΔPh* was plotted against ($N \times Mw$). Indeed, a good linearity was found between the two quantities (Fig. 4, inset), where *N* was calculated via SPR.

Specific protein binding to Abs

Results on the binding of protein molecules through a biotin linker highlight the importance of specific versus non-specific interaction. Additional verification comes from examining the data of a different type of specific interaction, that of an antibody-antigen, using as antigens four cardiac marker proteins. These proteins have been used before with the μF-on-SAW platform in order to demonstrate its validity in diagnostics.[41] When *ΔPh* derived from real time graphs (Fig. 2(c)) was plotted against *Mw*, it was found that the linearity holds again (Fig. 3(a), triangles), as in the case of the biotinylated molecules on neutravidin. Considering the experimental assay, monoclonal antibodies were used to capture the cardiac markers so this is an interaction of highly specific nature too. Although the biorecognition layer in this case consists of two layers (PrG and antibody), this does not seem to affect the linear response between *ΔPh* and *Mw*; this supports the idea that various kinds of specific binding can be used to control the number of attached proteins *N* at saturation.

The protein concentration parameter

The need to work at saturation conditions, i.e., have maximum binding site coverage, is exemplified in Fig. 6 where the *ΔPh*-*Mw* relationship is shown as concentration increases, when an antibody (Ab) is used as the capturing (receptor) molecule. Clearly, the linear relationship is established only at concentrations corresponding to the plateau of the adsorption isotherm for all examined antigens;[41] the same trend is seen for neutravidin (data shown in Figure S-3). Saturation is needed because it provides a unique solution to eqn (1) i.e., $deg \sim N \times Mw$; by adding a certain number of molecules you get an acoustic response which could just as well be obtained by a different number of molecules of a different weight. A unique determination of *Mw* requires fixing *N* and this happens only at maximum coverage ($N = N_{sat}$); N_{sat} is in turn determined by the receptor coverage of the sensor surface which is again predetermined, fixed (but can be modified) at the beginning of the experiment.

Quantitative interpretation of specific binding and physisorption

Our experimental results can be further used to derive some quantitative information, regarding the binding capacity of the two biorecognition surfaces, i.e., neutravidin and antibody-modified devices. Comparing the slopes of the acoustic responses (and keeping in mind that in these *ΔPh*-vs-*Mw* plots the slope of the trend line incorporates *N*) in Fig. 3(a) for the specific binding of proteins to neutravidin and antibodies, it can be seen that the latter is smaller than the former, suggesting a smaller number of molecule binding in the case where an antibody is used for the specific capturing. The linear fits are:

$$\Delta Ph_{Neu} = 0.016\, Mw + 0.5 \ (R^2 = 0.99) \quad (3)$$

$$\Delta Ph_{Ab} = 0.006\, Mw + 0.5 \ (R^2 = 0.99) \quad (4)$$

It can be seen that from eqns (3), (4), the experimental ± 0.2 deg error bar in phase measurements produces an equivalent in molecular weight of ± 12 kDa (at the level of ~100 kDa) and ±33 kDa (at the level of ~300 kDa) for the binding of the biotinylated and antigen proteins respectively; this amounts to a resolution of around 15%.

The above observation most likely reflects differences in the size of the receptor molecules (neutravidin and antibody) as compared to that of the incoming binding proteins, as well as differences in the spacing of the receptors on the surface. These geometrical constrains are discussed now. It is known that neutravidin adsorbs forming a layer where only two of its four biotin-binding sites are exposed to the bulk solution, the two sites being approximately 3 nm apart and the size of the whole molecule being ≈ 5 × 6 nm.[47] It has been shown that even in the case of a very slender cylinder like DNA (~2 nm wide) only about one biotinylated molecule can be anchored (per neutravidin) due to steric hindrance and electric repulsion.[25,48] Since the size of the proteins employed here is between 3 and 14 nm, it is safe to assume that a one-to-one binding is (at maximum) the most prevalent type of interaction. Given that the number of bound molecules (N_{sat}) is a constant for all four proteins and that BSA and IgG are larger than neutravidin, the conclusion is drawn that the neutravidins on the gold surface are not adjacent to each other but rather spaced apart. These constrains are not in effect for non-biotinylated proteins

[a] The acoustic ratio of energy dissipation per amount of adsorbed mass, i.e., *ΔA/ΔPh*, which is typically used to compare the viscoelasticity of different proteins, is found here to be between 0.022 and 0.040 dB/deg, the two extremes being protein A and IgG [46]. This means that the attached proteins exhibit a wide range of energy dissipation per unit mass (~2 fold), implying substantial differences in their viscoelastic properties.

adsorbing directly on gold where more space is available (and even more orientations of the molecules)[49] thus the adsorption process always leads to higher numbers of bound molecules than in the case of specific binding (compare Fig. 3(a,b) to Fig. 4). One could argue that this is observed because there exists a hidden parameter not factored-in in the analysis of the SAW data and/or in the assumption that ΔPh~mass without regard for the exact mode of interaction (protein/gold vs. protein/protein/gold). However, given that the same observation holds for the SPR data puts such a concern in doubt. The fact that the neutravidins are spaced apart is predicted by theoretical models (e.g. the random sequential adsorption model)[50,51] and is also supported by our data. A simple calculation shows that a full monolayer coverage, assuming a close-packed system, requires a surface mass density $m_{\text{monolayer}}$ given by:

$$m_{monolayer} \approx 1.67 \frac{Mw}{S} \quad (5)$$

where the molecular weight is in kDa, S the surface area/molecule in nm^2 and the result is in ng/mm^2 units. Inserting the data from Fig. 4 in eqn (2) we calculate that the surface coverage ($m_{sat}/m_{\text{monolayer}}$) by neutravidin is ≈ 60%; the error is at least 5% because the protein dimensions in the adsorbed state are not exactly known. Also assumed is that there are no aggregates adsorbing, something suspected at least for neutravidin.[52]

The same arguments can be applied to the set of data with the antibodies. These receptors also have to be spaced apart in order to accommodate the indeed much larger cardiac markers if again a constant N parameter is to be justified. This requirement is probably satisfied, as for neutravidin, since the calculated surface coverage for protein G is ≈ 27% so the immobilized antibodies are even more sparse. The difference in surface coverage in the two systems can also be inferred by another way. Using eqns (3), (4) we can derive a graph depicting the ratio of N_{Neu} bound on neutravidin over N_{Ab} bound on antibody (Fig. 3(a), inset). At very small values of Mw (≈ 0) both receptors have the same capacity, i.e., N_{Neu} / N_{Ab} ≈ 1; extrapolation to the highest Mw common between the two lines (i.e., 150 kDa) shows that the neutravidin-modified surface is able to bind (at a minimum) approximately two times more molecules than the antibody-modified one. This constitutes evidence that the spacing of the antibodies (on PrG) is more than double the corresponding one for neutravidin (on Au). This gap indeed exists, as the surface coverage numbers indicate, and although not needed in the case of relatively small incoming proteins it is essential for bigger ones.

Conclusions

This work reports for the first time that the phase change of an acoustic sensor is proportional to the molecular weight of specifically bound proteins, a result also confirmed via an SPR biosensor. In principle, other modes of acoustic sensors (e.g. thickness shear/QCM) could be used besides the Love mode employed here. This holds true in those cases where the surface is saturated with the specifically bound proteins, regardless of their Mw (within the range of 30 to 540 kDa) and the type of biorecognition receptor used (neutravidin or antibodies). The effect was attributed to the same number of molecules specifically binding to their receptors, as opposed to those molecules that simply physisorb on gold. The results imply that even at high surface coverage, the acoustic signal can be used to derive information related to intrinsic properties of the bound analyte and the acoustic device can work as a potential method to determine the Mw of molecules with a resolution of ~15%. The method can be used to accurately determine protein Mw in those applications where western blotting or electrophoresis is typically applied. Given that a typical electrophoresis gel has a resolution of ~ 5 kDa (at the level of ~50 kDa) or ~ 10 %, our result compares favorably. Applications include the isolation and identification of genetically produced proteins which carry a specific tag for capturing and purification; by using a functionalized surface selective for this tag, the presence and integrity of the produced protein could be identified in an easy and fast manner, by simply monitoring the phase signal. In addition, specific antibodies could be used in combination with the μF-on-SAW system to screen for the presence of different proteins in one sample. Again, phase measurements could be used to verify, not only the presence of each protein through Ab-binding, but also accurately confirm if the protein exists as a monomer/dimer etc. or as an aggregate.

Acknowledgements

K.M acknowledges the Public Benefit Foundation "Alexander S. Onassis", A.T the EU-*FP7* grant: REGPOT-"InnovCrete" (Contract No: 316223) and E.G the EU-*FP7* grant: "Love-Food" (Contract No: 317742) for financially supporting this work.

Notes and references

[a] *Institute of Molecular Biology & Biotechnology, Foundation for Research & Technology Hellas, 100 N. Plastira Street, GR-70013 Heraklion, Greece; Fax: +30 2810 394408; Tel: +30 2810 304373; E-mail: gizeli@imbb.forth.gr and atsortos@imbb.forth.gr*
[b] *Department of Materials Science & Technology, University of Crete, Vassilika Vouton, GR-71003 Heraklion, Greece*
[c] *Department of Biology, University of Crete, Vassilika Vouton, GR-71409 Heraklion, Greece*
[§] *Current address: Laboratory for MEMS Applications, Department of Microsystems Engineering (IMTEK), University of Freiburg & HSG-IMIT - Institut für Mikro- und Informationstechnik, Georges-Koehler-Allee 103, 79110 Freiburg, Germany*
† Electronic Supplementary Information available

References

1 R. McKendry, J. Zhang, Y. Arntz, T. Strunz, M. Hegner, H.P. Lang, M.K. Baller, U. Certa, E. Meyer, H.-J. Güntherodt and Ch. Gerber, *Proc. Natl. Acad. Sci. U.S.A.*, 2002, **99**, 9783-9788.

2 M. Pohanka and P. Skládal, *J. Appl. Biomed.*, 2008, **6**, 57-64.

3 X. Fan, I.M. White, S.I. Shopova, H. Zhu, J.D. Suter and Y. Sun, *Anal. Chim. Acta*, 2008, **620**, 8-26.

4 S.J. Martin, G.C. Frye and S.D. Senturia, *Anal. Chem.*, 1994, **66**, 2201-2219.

5 D.S. Ballantine, R.M. White, S.J. Martin, A.J. Ricco, E.T. Zellers, G.C. Frye and H. Wohltjen, Acoustic Wave Sensors, 1997, Academic Press, San Diego, CA.

6 A.J. Ricco and S.J. Martin, *Appl. Phys. Lett.*, 1987, **50**, 1474-1476.

7 A. Saluja, A.V. Badkar, D.L. Zeng, S. Nema and D.S. Kalonia, *Biophys. J.*, 2007, **92**, 234-244.

8 N.B. Eisele, F.I. Andersson, S. Frey and R.P. Richter, Biomacromolecules, 2012, **13**, 2322-2332.

9 F. Josse, F. Bender and R.W. Cernosek, *Anal. Chem.*, 2001, **73**, 5937-5944.

10 K. Länge, B.E. Rapp and M. Rapp, *Anal. Bioanal. Chem.*, 2008, **391**, 1509-1519.

11 T.M.A. Gronewold, *Anal. Chim. Acta*, 2007, **603**, 119-128.

12 P.M. Wolny, J.P. Spatz and R.P. Richter, *Langmuir*, 2010, **26**, 1029-1034.

13 G.N.M. Ferreira, A.C. Da-Silva and B. Tome, *Trends Biotechnol.*, 2009, **27**, 689-697.

14 R.E. Speight and M.A. Cooper, *J. Mol. Recognit.*, 2012, **25**, 451-473.

15 K.A. Melzak, F. Bender, A., Tsortos and E. Gizeli, *Langmuir*, 2008, **24**, 9172-9180.

16 I. Reviakine, M. Gallego, D. Johannsmann and E. Tellechea, *J. Chem. Phys.*, 2012, **136**, 084702.

17 H.W. Ma, J.A. He, Z.Q. Zhu, B.E. Lv, D. Li, C.H. Fan and J. Fang, *Chem. Commun.*, 2010, **46**, 949-951.

18 I. Reviakine, D. Johannsmann and R.P. Richter, *Anal. Chem.*, 2011, **83**, 8838-8848.

19 D. Johannsmann, *Phys. Chem. Chem. Phys.*, 2008, **10**, 4516-4534.

20 W.Y.X. Peh, E. Reimhult, F.T. Huey, J.S. Thomsen and X. Su, *Biophys. J.*, 2007, **92**, 4415-4423.

21 H.-S. Lee, M. Contarino, M. Umashankara, A. Schön, E. Freire, A.B. Smith III, I.M. Chaiken and L.S. Penn, *Anal. Bioanal. Chem.*, 2010, **396**, 1143-1152.

22 X.M. Wang, J.S. Ellis, E.L. Lyle, P. Sundaram and M. Thompson, *Mol. Biosyst.*, 2006, **2**, 184-192.

23 J.S. Ellis and M. Thompson, *Chem. Sci.*, 2011, **2**, 237-255.

24 M. Huang, J.A. He, J.H. Gan and M.W. Ma, *Colloid Surface B*, 2011, **85**, 92-96.

25 A. Tsortos, G. Papadakis, K. Mitsakakis, K. Melzak and E. Gizeli, *Biophys. J.*, 2008, **94**, 2706-2715.

26 G. Papadakis, A. Tsortos and E. Gizeli, *Nano Lett.*, 2010, **10**, 5093-5097.

27 G. Papadakis, A. Tsortos and E. Gizeli, *Biosens. Bioelectron.*, 2009, **25**, 702-707.

28 G. Papadakis, A. Tsortos, F. Bender, E.E. Ferapontova and E. Gizeli, *Anal. Chem.*, 2012, **84**, 1854-1861.

29 G. Papadakis, A. Tsortos, A. Kordas, I. Tiniakou, E. Morou, J. Vontas, D. Kardassis and E. Gizeli, *Sci. Rep.*, 2013, **3**, 2033.

30 T. Ozeki, M. Morita, H. Yoshimine, H., Furusawa and Y. Okahata, *Anal. Chem.*, 2007, **79**, 79-88.

31 F. Höök, B. Kasemo, T. Nylander, C. Fant, K. Sott and H. Elwing, *Anal. Chem.*, 2001, **73**, 5796-5804.

32 N. Weber, A. Pesnell, D. Bolikal, J. Zeltinger and J. Kohn, *Langmuir*, 2007, **23**, 3298-3304.

33 M. Weiss, W. Welsch, M. von Schickfus and S. Hunklinger, *Anal. Chem.*, 1998, **70**, 2881-2887.

34 L.A. Francis, J.M. Friedt, C. Zhou and P. Bertrand, *Anal. Chem.*, 2006, **78**, 4200-4209.

35 F. Bender, P. Roach, A. Tsortos, G. Papadakis, M.I. Newton, G. McHale and E. Gizeli, *Meas. Sci. Technol.*, 2009, **20**, 124011.

36 A. Rasmusson and E.Gizeli, *J. Appl. Phys.*, 2001, **90**, 5911-5914.

37 K. Mitsakakis, A. Tsortos, J. Kondoh and E. Gizeli, *Sens. Actuat. B, Chem.*, 2009, **138**, 408-416.

38 J.C. McDonald, D.C. Duffy, J.R Anderson, D.T. Chiu, H. Wu, O.J.A. Schueller and G.M. Whitesides, *Electrophoresis*, 2000, **21**, 27-40.

39 K. Mitsakakis, A. Tserepi and E. Gizeli, *J. Microelectromech. Syst.*, 2008, **17**, 1010-1019.

40 K. Mitsakakis and E. Gizeli, *Biosens. Bioelectron.*, 2011, **26**, 4579-4584.

41 K. Mitsakakis and E. Gizeli, *Anal. Chim. Acta*, 2011, **699**, 1-5.

42 G. Sauerbrey, *Zeitschrift Phys.*, 1959, **155**, 206-222.

43 J. Vörös, *Biophys J.*, 2004, **87**, 553-561.

44 M.B. Hovgaard, K. Rechendorff, J. Chevallier, M. Foss and F. Besenbacher, *J. Phys. Chem. B*, 2008, **112**, 8241-8249.

45 E. Steinberg, B. Persson, H. Roos and C. Urbaniczky, *J. Colloid. Interf. Sci.*, 1991, **143**, 513-526.

46 K. Mitsakakis, A. Tsortos, E. Gizeli, manuscript in preparation.

47 C. Rosano, P. Arosio and M. Bolognesi, *Biomol. Eng.*, 1999, **16**, 5-12.

48 C. Larsson, M. Rodahl and F. Höök, *Anal. Chem.*, 2003, **75**, 5080-5087.

49 M.E. Wiseman and C.W. Frank, *Langmuir*, 2012, **28**, 1765-1774.

50 J.W. Evans, *Rev. Mod. Phys.*, 1993, **65**, 1281-1329.

51 E.A. Vogler, *Biomaterials*, 2012, **33**, 1201-1237.

52 P.M. Wolny, J.P Spatz and R.P. Richter, *Langmuir*, 2010, **26**, 1029-1034.

Figures

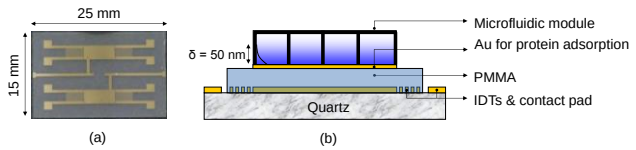

Fig. 1. (a) Image of a dual-SAW sensor chip. (b) Side view of the μF-on-SAW configuration with the microfluidic module (black) dividing the total sensing area into four domains.

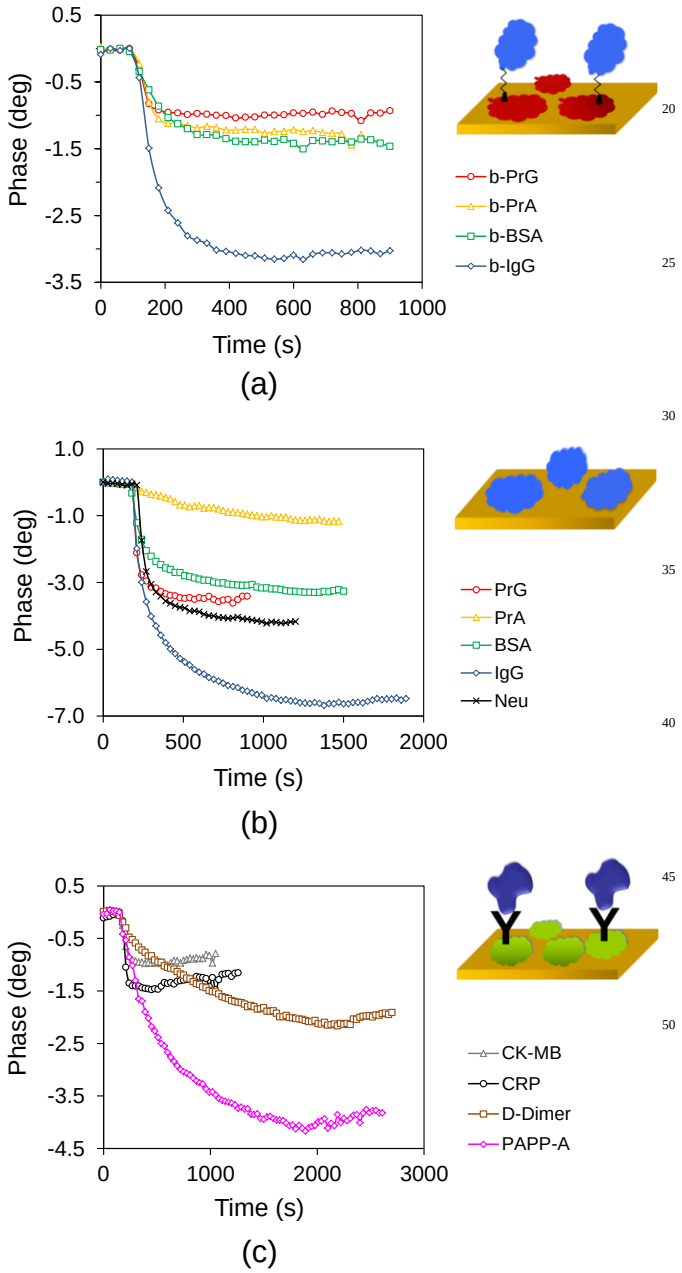

Fig. 2. Real-time phase for the three sets of examined biomolecules together with a schematic representation of their binding on the sensor surface: (a) biotinylated molecules specifically binding on a (preformed) neutravidin (red) layer; (b) non-biotinylated molecules directly adsorbing on gold; (c) cardiac biomarkers specifically binding to their homologous antibodies (the antibodies are themselves also specifically bound on a PrG (green) layer).

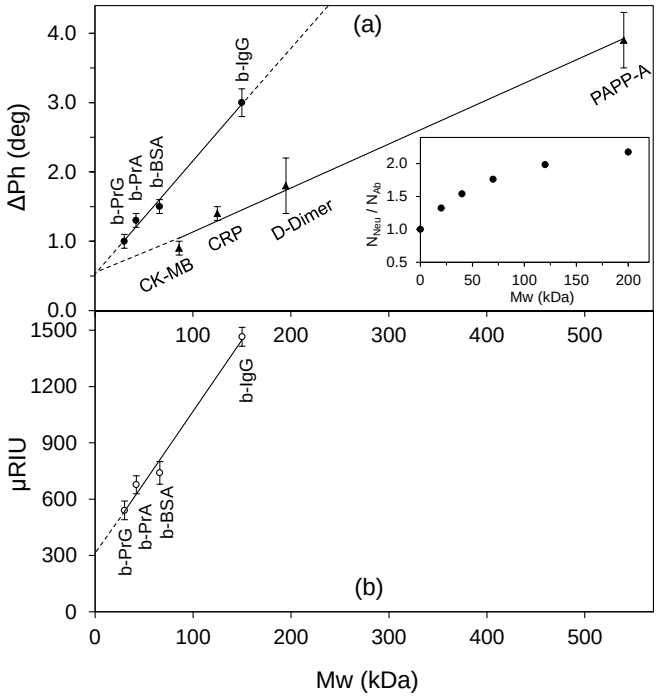

Fig. 3. Linear relation of SAW (a) and SPR (b) signal vs. molecular weight; biotinylated molecules specifically bound to neutravidin (filled circles for SAW in (a), open circles for SPR in (b)); cardiac markers specifically bound to their homologous antibodies (filled triangles in (a)). Inset in (a): ratio of N_{Neu} / N_{ab} vs. *Mw, where* N_{Neu} and N_{Ab} indicate number of molecules bound on neutravidin and antibody, respectively; this ratio indicates the different binding capacity of neutravidin and antibodies.

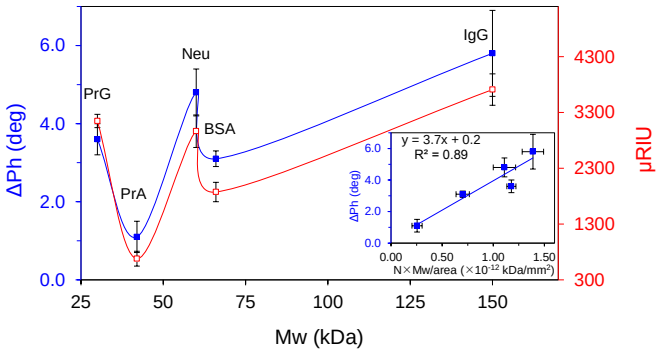

Fig. 4. Non-linear relation of SAW and SPR signals vs. the molecular weight of non-biotinylated molecules directly adsorbed on gold; the inset shows the transformation of the non-linear relation into linear when ΔPh is plotted vs. $N \times Mw$.

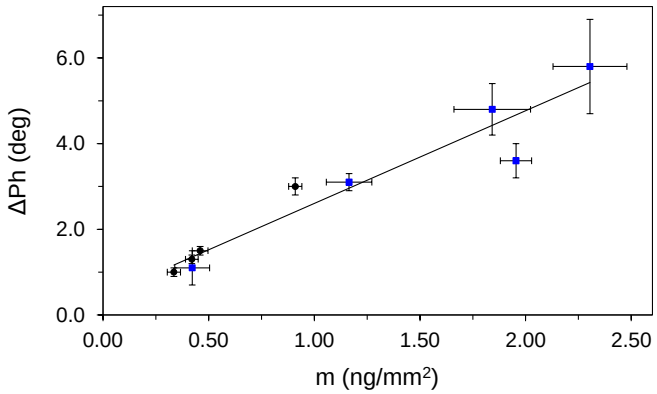

Fig. 5. Correlation of acoustic signal to mass per area (calculated via SPR) using data acquired from the biotinylated (filled black circles) and non-biotinylated molecules (filled blue squares).

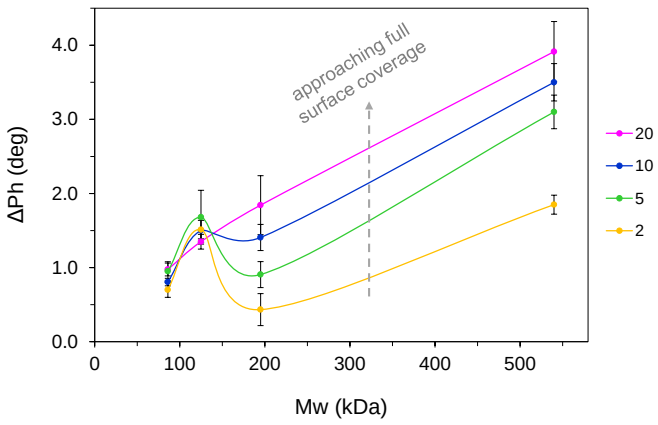

Fig. 6. Phase change vs. molecular weight as concentration (in µg/ml) increases for the specific binding of cardiac markers to their homologous antibodies.